Proceedings of "Applications of Physics in Mechanical and Material Engineering" (APMME 2023)

Influence of a Small Addition of Cu on the Magnetization Process of Rapid Quenched Alloys in Strong Magnetic Fields

B. Jeż[a], P. Postawa[a], A. Kalwik[a], M. Nabiałek[b], J. Gondro[b] and M.M. Nabiałek[b]

[a] *Department of Technology and Automation, Faculty of Mechanical Engineering and Computer Science, Czestochowa University of Technology, al. Armii Krajowej 19c, 42-200 Częstochowa, Poland*
[b] *Department of Physics, Faculty of Production Engineering and Materials Technology, Czestochowa University of Technology, al. Armii Krajowej 19, 42-200 Częstochowa, Poland*

Doi: 10.12693/APhysPolA.144.325 *e-mail: bartlomiej.jez@pcz.pl

The magnetization process is based on bringing about a unified arrangement of the magnetic domains. During this process, there are shifts and then the rotations of the domain walls. At a later stage, domains with a direction of magnetization that do not correlate with the applied magnetic field disappear. The turnover depends on the size of the domains. For an amorphous structure, the key factors determining the size of the magnetic domains are the distance between the magnetic atoms and the possible presence of crystalline grains. The paper presents the results of research on the influence of Cu addition on the distances between magnetic atoms and the magnetization process in high magnetic fields. The structure of the alloys was studied using X-ray diffraction. The mean grain size was estimated using the Scherrer method. The magnetic properties were determined on the basis of measurements with a vibrating magnetometer. A numerical analysis of the primary magnetization curves was performed. Despite the significant reorganization of the structure, no changes in the distance between the magnetic atoms were observed, as indicated by slight changes in the D_{spf} parameter. It was found that a small addition of Cu positively influences the improvement of the magnetic properties, in particular the reduction of the value of the coercive field.

topics: Cu addition, nanocrystallization, Curie temperature, soft magnetic properties

1. Introduction

Rapid quenched alloys with a high Fe content are characterized by good magnetic properties. Depending on the cooling rate and chemical composition, it is possible to produce alloys with an amorphous or nanocrystalline structure in a one-stage process [1]. The type of phases formed during solidification determines the properties of these materials — rapid quenched alloys may have hard magnetic properties (for example, with the $Y_2Fe_{14}B$ phase [2]), semi-hard magnetic properties (with the Fe_5Y phase [3]), or soft magnetic properties (with the α-Fe, Fe_2B, $Fe_{23}B_6$, Fe_3B [4–6]). The properties of these alloys are related, among other things, to the distances between magnetic atoms [7] and the size of crystal grains [8].

Designing an alloy with good soft magnetic properties in a one-step process is quite a difficult task. Additions of some transition metals in amounts below 1% cause very large changes in the alloy's glass-forming ability [9–12]. Appropriate selection of the chemical composition allows obtaining a nanocrystalline alloy with phases improving soft magnetic properties.

The aim of the work is to determine the effect of Cu addition on the structure and magnetic properties of rapidly quenched FeCo-based alloys.

2. Experimental procedure

Polycrystalline alloy ingots were produced in an arc furnace under a protective atmosphere of argon (Ar pressure 0.3 atm). The alloys were melted from high-purity ingredients: B — 99.9%, other ingredients — 99.99%. The melting process was carried out on a copper plate cooled by water. The charge was melted 5 times, and the ingot was turned over each time to homogenize it. The ingots were cleaned mechanically and, after being divided into smaller pieces, in an ultrasonic bath. Samples of

rapid quenched alloys were produced by the injection method. Plate-shaped samples with dimensionss of $10 \times 10 \times 0.5$ mm^3 were obtained. The injection process was carried out in a protective atmosphere of argon (Ar pressure 0.3 atm).

The structure of the alloys was examined using X-ray diffraction (XRD). A Bruker ADVANCE 8 diffractometer was used. Measurements were carried out with a measuring step of 0.02° and an exposure time of 5 s. The measured diffractograms were analyzed using the Match! program. The data obtained from the analysis were used to determine the average grain sizes using the Scherrer method [13]

$$D = \frac{\lambda K}{2\beta_0 \cos(\theta)}, \quad (1)$$

where:

K — Scherrer form factor ($K = 0.91$),

λ — wavelength of characteristic radiation,

β_0 — half width at half peak intensity (background included),

θ — Bragg's angle.

Static magnetic hysteresis loops and primary magnetization curves were measured using a Lake Shore VSM 7307 vibration magnetometer in the range of external magnetic field intensity up to 2 T. Based on the analysis of the primary magnetization curve, the spin wave stiffness parameter D_{spf} was calculated. For this purpose, the direction parameter of the line, b, should be determined, which fits the magnetization course as a function of $(\mu_0 H)^{1/2}$, where H is the external magnetic field. The b parameter is related to the spin wave stiffness parameter by the relationship [7]

$$b = 3.54\, g\mu_0\mu_\mathrm{B} \left(\frac{1}{4\pi D_{spf}}\right)^{3/2} k_\mathrm{B} T\, (g\mu_\mathrm{B})^{1/2}, \quad (2)$$

where:

b — slope of the linear fit corresponding to the thermally-induced suppression of spin-waves by a magnetic field of high intensity,

μ_0 — magnetic permeability of a vacuum,

k_B — Boltzmann's constant,

μ_B — Bohr magneton,

g — gyromagnetic factor,

T — temperature.

3. Results

Figure 1 presents X-ray diffraction images obtained for the tested alloys in the solidified state.

The measured diffractograms differ significantly from each other. The $Fe_{36}Co_{36}Y_8B_{20}$ alloy is characterized by an amorphous structure, as indicated by the presence of a single wide, diffuse maximum (Fig. 1a). The minimal addition of Cu caused partial crystallization of the alloy during its solidification. The presence of crystalline phases α-Fe and

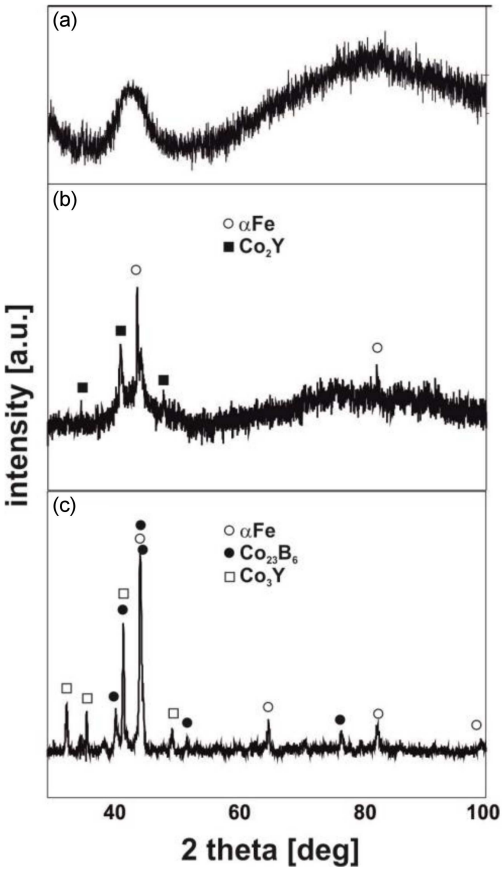

Fig. 1. X-ray diffraction patterns for the rod-form samples of the investigated alloys: (a) $Fe_{36}Co_{36}Y_8B_{20}$, (b) $(Fe_{36}Co_{36}Y_8B_{20})_{99.9}Cu_{0.1}$, (c) $(Fe_{36}Co_{36}Y_8B_{20})_{99}Cu_1$.

TABLE I

Results of analysis for XRD measured for the tested alloys.

Alloy	Medium grain size [nm]			
	Co_2Y	α-Fe	$Co_{23}B_6$	Co_3Y
$(Fe_{36}Co_{36}Y_8B_{20})_{99.9}Cu_{0.1}$	18	32	–	–
$(Fe_{36}Co_{36}Y_8B_{20})_{99}Cu_1$	–	22	20	18

Co_2Y was identified (Fig. 1b). In this case, the maximum indicating the presence of a disordered phase is still very clear. Together with the low intensity of the peaks, this indicates a small share of crystals in the melt volume. An alloy with 1% copper is much more crystallized. Co_3Y, α-Fe, and $Co_{23}B_6$ phases were identified in the sample volume. The maximum associated with the amorphous phase is barely noticeable. Based on the diffractograms, average grain sizes were determined for the tested alloys. The results are given in Table I.

For all identified phases, the grain size does not exceed 35 nm. Taking into account the type of phases present in the alloys, it should be assumed that they should not have a negative impact on the soft magnetic properties of the tested alloys.

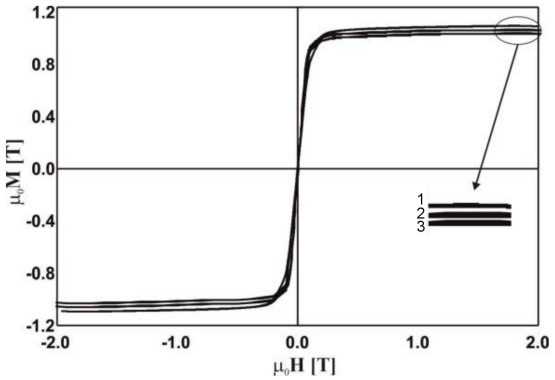

Fig. 2. Static magnetic hysteresis loops for the tested alloy samples: (a) $Fe_{36}Co_{36}Y_8B_{20}$, (b) $(Fe_{36}Co_{36}Y_8B_{20})_{99.9}Cu_{0.1}$, (c) $(Fe_{36}Co_{36}Y_8B_{20})_{99}Cu_1$.

TABLE II

Magnetic properties of investigated alloys.

	M_S [T]	H_C [A/m]	D_{spf} [meV nm^2]	Phases
$Fe_{36}Co_{36}Y_8B_{20}$ [14]	1.09	208	51	amorp.
$(Fe_{36}Co_{36}Y_8B_{20})_{99.9}Cu_{0.1}$	1.03	74	49	α-Fe, Co_2Y
$(Fe_{36}Co_{36}Y_8B_{20})_{99}Cu_1$	1.07	185	51	α-Fe, Co_3Y, $Co_{23}B_6$

Figure 2 shows static magnetic hysteresis loops for the produced alloy samples. The measured loops have a shape typical for soft magnetic materials. On the basis of the loop, the saturation magnetization value (M_S) and the value of the coercive field (H_C) were determined; the data are presented in Table II (see also [14]).

Figure 3 shows the magnetization curves as a function of $(\mu_0 H)^{1/2}$. The primary magnetization curves were subjected to numerical analysis. On its basis, the spin wave stiffness parameter D_{spf} was determined (Table II).

It turns out that the presence of crystalline phases does not affect the distances between magnetic atoms, moreover, the presence of only two crystalline phases (alloy $(Fe_{36}Co_{36}Y_8B_{20})_{99.9}Cu_{0.1}$) significantly reduces the H_C value. The presence of three crystalline phases complicates the magnetic structure and, to some extent, hinders the process of magnetizing the alloy. This may be related to the obstruction of the rotation of the domain walls by one of the crystalline phases present.

4. Conclusions

The work showed that even 0.1% of Cu addition reduces the alloy's glass-forming ability. With a 1% addition, this effect is much more visible.

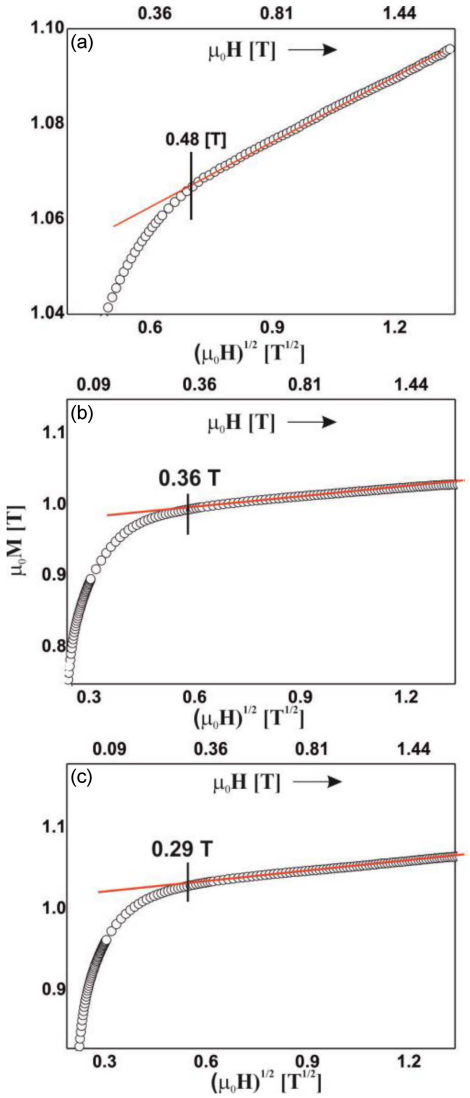

Fig. 3. Magnetization as a function of $(\mu_0 H)^{1/2}$ for the investigated alloys: (a) $Fe_{36}Co_{36}Y_8B_{20}$, (b) $(Fe_{36}Co_{36}Y_8B_{20})_{99.9}Cu_{0.1}$, (c) $(Fe_{36}Co_{36}Y_8B_{20})_{99}Cu_1$.

A small addition of Cu resulted in the formation of two crystalline phases, while a larger addition resulted in three phases. The magnetization process of all tested alloys is similar, but the alloy $(Fe_{36}Co_{36}Y_8B_{20})_{99.9}Cu_{0.1}$ shows the best magnetic properties. Due to the similar average grain size for nanocrystalline alloys, it should be stated that this effect is related to the less complicated magnetic structure of the $(Fe_{36}Co_{36}Y_8B_{20})_{99.9}Cu_{0.1}$ alloy.

References

[1] B. Jeż, K. Błoch, J. Gondro, K. Jeż, M. Talar, B. Płoszaj, P. Pietrusiewicz, S. Walters, A. Kalwik, D.S. Che Halin, P. Sikora, M. Nabiałek, *Acta Phys. Pol. A* **139**, 495 (2021).

[2] P. Vizureanu, M. Nabiałek, A.V. Sandu, B. Jeż, *Materials* **13**, 835 (2020).

[3] S.S. Chandrasekaran, M.R. Ponnaiah, P. Murugan, P. Saravanan, *J. Magn. Magn. Mater.* **418**, 92 (2016).

[4] L. Zhang, Z. Wang, Y. Jia, *Mater. Sci. Eng. B* **231**, 1 (2018).

[5] H.Y. Jung, S. Yi, *Intermetallics* **49**, 18 (2014).

[6] M.E. McHenry, F. Johnson, H. Okumura, T. Ohkubo, V.R.V. Ramanan, D.E. Laughlin, *Scr. Mater.* **48**, 881 (2003).

[7] T. Holstein, H. Primakoff, *Phys. Rev.* **59**, 388 (1941).

[8] Y. Li, X Jia, W. Zhang, Y. Zhang, G. Xie, Z. Qiu, J. Luan, Z. Jiao, *J. Mater. Sci. Technol.* **65**, 171 (2021).

[9] Y. Zhang, Y. Wang, A. Makino, *AIP Adv.* **8**, 047703 (2018).

[10] Z. Jaafari, A. Seifoddini, S. Hasani, *Metall. Mater. Trans. A* **50A**, 2875 (2019).

[11] X. Jia, Y. Li, G. Xie, T. Qi, Zhang, *J. Non-Cryst. Solids* **481**, 590 (2018).

[12] W. Lin, Y.Z. Yang, J. Xu, W. Li, *J. Alloys Compd.* **735**, 1195 (2018).

[13] G.T. Xia, Y.G. Wang, J. Dai, Y.D. Dai, *J. Alloys Compd.* **690**, 281 (2017).

[14] K. Błoch, M. Nabiałek, P. Postawa, A.V. Sandu, A. Śliwa, B. Jeż, *Materials* **13**, 846 (2020).